

in a stereo image pair means that the correspondence problem is principally solved for the object.

The overall algorithm design can be seen in figure 1. In order to enable an automatic extraction of the z-position and the position in the image plane, we developed a recognition algorithm able to detect the objects used in our experiments and deliver the necessary initialization data for the tracking algorithm. The tracking algorithm is split into separate algorithms for each stereo pair image. The tracker for the left image is in the first place minimized freely to segment the object from the background. The contour data is then duplicated to the right image tracker, which uses just restricted transformations to determine the position of the object in the right image. Both position informations are fed to a depth estimation algorithm, which analyzes the displacement of the two tracked positions and determines the distance of the object.

2 ALGORITHM INITIALIZATION

A common drawback of active contour based approaches is the necessity for manual algorithm initialization. Usually a graphical user interface (GUI) is used to present a dialog where the user is asked to draw an initial estimate of the object's shape. Instead we choose another approach which allows automatic initialization of the active contour. The proposed method is based on the very popular edge detection method of Canny (Gonzalez and Woods, 2008) and an initial estimate of the object size. In the following we will give a brief overview of Canny edge detection and then show how it can be applied to our problem.

To reduce the effect of high frequency noise usually a Gaussian low-pass filter is applied to the input image before edge detection. The main advantages of the Gaussian low-pass are the efficient computability and the good stopband attenuation (Forsyth and Ponce, 2002). The convolution kernel is:

$$G_{\sigma}(x, y) = \frac{1}{2\pi\sigma^2} \exp\left(-\frac{(x^2 + y^2)}{2\sigma^2}\right) \quad (1)$$

The actual contour detection algorithm consists of the following steps:

1. *Determination of edge points* - A measure of image gradient G in the direction of the image coordinate axes x, y is needed. The Sobel- and Prewitt operator (Jaehne, 1991) are two examples of first-order derivative approximation filters. From the filter responses G_x, G_y the local gradient magnitude $g(x, y)$ and orientation $\alpha(x, y)$ are computed:

$$g(x, y) = \sqrt{G_x^2 + G_y^2} \quad (2)$$

$$\alpha(x, y) = \tan^{-1}(G_y/G_x) \quad (3)$$

Edge points are obtained by finding the local maxima of $g(x, y)$ in the direction of $\alpha(x, y)$.

2. *Nonmaximal suppression* - The prior step produces ridges along image edges that are not yet necessarily a thin line. Nonmaximal suppression removes pixels that are not on the top of the ridge and leaves a thin line.
3. *Hysteresis thresholding* - Two threshold values T_1 and T_2 , with $T_1 < T_2$ are used to remove edges of low strength. Initially, all edge pixels where $g(x, y) < T_1$ are removed. The next step removes all remaining pixels with $T_1 < g(x, y) < T_2$ that are not 8-connected to an edge segment with $g(x, y) > T_2$. This procedure is depicted in figure 2.

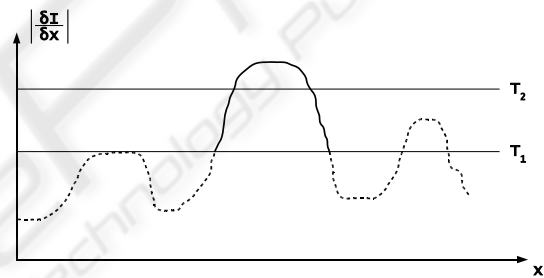


Figure 2: Hysteresis thresholding as used in Canny edge detection, illustrated by a one-dimensional signal I . Only connected line segments with derivative values higher than T_1 and at least one segment higher than T_2 survive this step.

The methods as described above have been applied to a sample SEM image taken from the automation sequence (figure 3). The Sobel operator has been chosen as edge emphasizing filter. It can be seen from the result of the Canny edge detection that is not only sensitive to the target object but also to background structure. For retrieving the actual object shape that is used to initialize the active contour we incorporate three further steps:

4. *Binary dilation* - Lines in the binary edge image are thickened to close gaps in the outer object hull. For this operation a *structuring element* is needed which is another binary image. A binary approximation of a circular disk is a common choice.
5. *Contour retrieval* - The dilated image is inspected for contours which are point sequences that enclose 8-connected binary objects. Only outer contours which are not wrapped by a larger contour are taken into account.

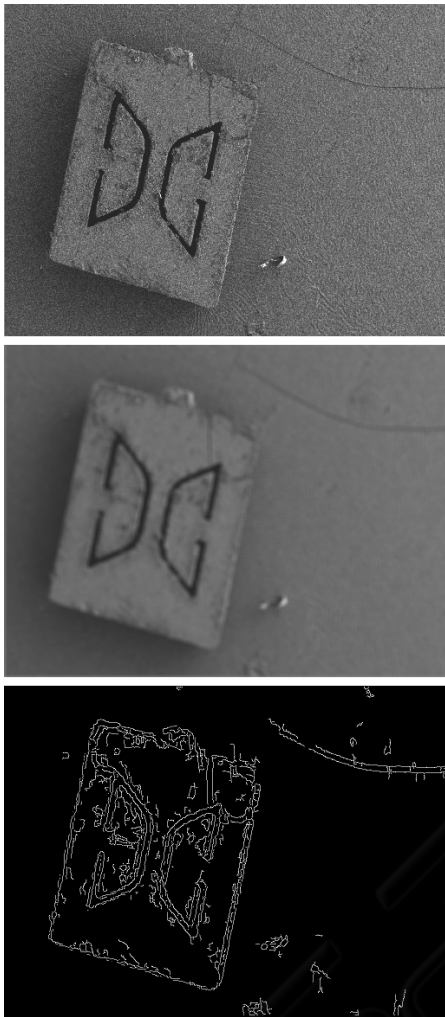


Figure 3: Processing steps: the initial image (top) after Gaussian filtering (middle) and Canny edge detection (bottom).

6. *Size thresholding* - From the outer object contours the enclosed area and thus the object mass can be derived directly. In this particular problem setting the object in demand is the largest object in the image scene. Also the physical dimensions are well-known. All but the largest object are dropped.

These processing steps have been applied to the output of the edge detection and the results can be seen in figure 4. The dilated image (top) points out and connects the image edges. Outer contours are detected and the enclosed regions are filled (middle image, overlaid with the original image). Finally small objects are removed from the image scene (bottom). The object boundary pixels are output of the initialization procedure and input to the active contour algorithm.



Figure 4: Binary dilation with a circular structuring element is applied (top). After region growing (middle), objects which do not meet the expected size are removed (bottom).

3 OBJECT TRACKING

In order for generating input data for the depth estimation, a tracking algorithm is used to track the position of the object not only in one image, but separately in the two stereo images. The tracking algorithm is based on active contours (for details on this concept see (Kass et al., 1988) and (Blake and Isard, 2000)). Active contours are curves in the image plane which segment the image into two regions, one enclosed by the contour and one surrounding the contour. The enclosed segment is the tracked object, the surrounding segment the rest of the scene. For determining the segmentation, active contours exhibit an energy function. This energy function is dependent on certain properties of the contour, like length, com-

compactness etc., and on properties of the image data, like edges.

Though the original formulation of the active contours like described in (Kass et al., 1988) depends on edges for the energy function, it turned out that an energy function derived from image region statistics is more robust for SEM images (for details see (Sievers, 2006) and (Sievers, 2007)). Especially this is the case with very noisy images. The energy function used here is defined as

$$E(C) = E_{int}(C) + E_{ext}(C) \quad (4)$$

with

$$E_{int}(C) = \frac{L^3}{A} \quad (5)$$

with L the length of the contour, A the area enclosed by the contour and

$$E_{ext}(C) = N_a f\left(\frac{1}{N_a} \sum_{x \in a} x\right) + N_b f\left(\frac{1}{N_b} \sum_{x \in b} x\right) \quad (6)$$

with

$$f(z) = -z \ln(z) \quad (7)$$

with a and b being the two regions in which the contour segments the image.

The original algorithm has been used already for the tracking of objects in SEM images. Important in comparison to microscope is that the algorithm has to be as robust as possible against certain effects which may occur in SEM images, especially in SEM nanomanipulations setups. It has shown to be robust against:

- *noise - due to fast SEM image acquisition during manipulation*
- *partial occlusion - due to complex manipulation setups*
- *grey level fluctuations - due to charge accumulation and discharging effects in the SEM chamber*

The implementation is fast enough to track objects in SEM images with relatively high framerates. For the initial minimization, the contour points are handled individually, resulting in a deforming contour which fits itself to the object. After the initial minimization of the contour, the transformation for the subsequent steps is restricted to euclidean transforms. This enables the left image tracker to transfer the contour points to the right image tracker, and is also the reason for the robustness against occlusion. The transfer and duplication of the contour leads to the same object being tracked in both stereo images.

The steps executed in the minimization of the whole contour are the following, executed in order:

1. *Minimization by translation in X*

2. *Minimization by translation in Y*

3. *Minimization by rotation*

In the original algorithm (described in (Sievers, 2007)), additional minimization by scaling was executed, which is not used here due to coherency issues. When adding the scaling minimization, the tracking gets slightly more unstable, and a independent minimization on the two separate images may lead to incoherent states of the tracker, e.g. different scaling factors for the two images.

The modifications made to the algorithm mainly deal with the duplication of the tracker for stereo tracking. The left image tracker is extended with a component duplicating the contour like shown in figure 5, the right image tracker does not need an own free minimization of the contour, but is initialized by the left image tracker with the contour data as shown in figure 6.

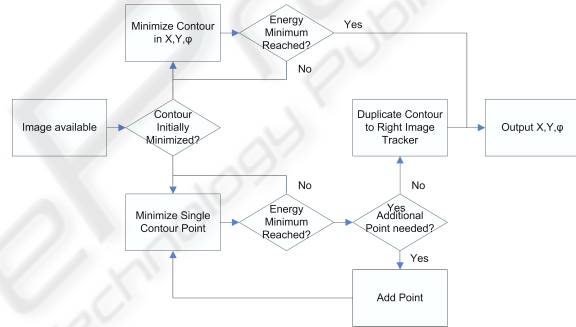


Figure 5: The tracking algorithm for the left image.

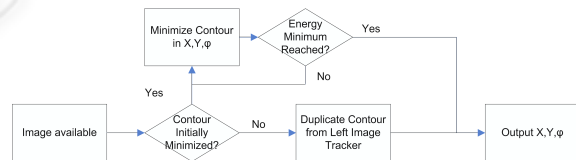


Figure 6: The tracking algorithm for the right image.

The active contour tracker itself is robust enough to track the objects in the experiment, though some parameter tuning was necessary due to the inhomogeneous appearance of the objects.

4 DEPTH ESTIMATION

Many modern applications use the well known advantages of SEMs. These applications often require knowledge of the exact position of involved objects or topographic information of a specimen. Therefore, measurements for all 3 dimensions are required. This requirement exceeds the possibilities of standard

SEMs, because they are only capable of delivering 2-dimensional images of a scene. Typical applications are grabbing and assembling processes such as the manipulation of carbon nanotubes (CNT).

There are different approaches to obtain 3-dimensional measurements in scanning electron microscopy. Beside tactile sensors and laser-based measuring methods, focus-based methods are popular in image processing. Due to problems with the standard methods over the last years stereoscopy-based methods in SEM applications gained in importance. The advantage of stereoscopy techniques is the ability to display dynamic processes in real time in contrast to focus-based methods which need to acquire a series of images for depth calculation.

The application of the stereoscopy principle in the SEM is similar to the application in the macro world. Different z-positions lead to different displacements between the two stereo images. This displacement leads to z-position dependent disparities of the corresponding points. The disparity is used to calculate the original z-position. The angular displacement between the two views is also called vergence angle (figure 7).

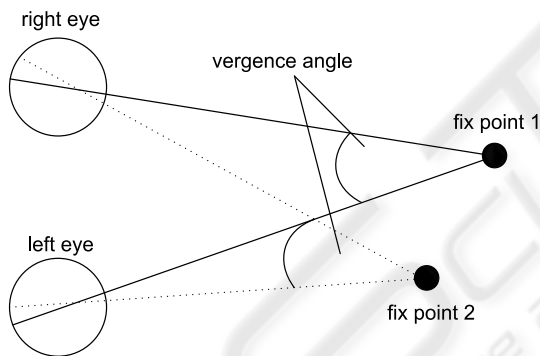


Figure 7: The principle of stereoscopy using the example of human vision.

The stereoscopy approach consists of two main parts: the stereo image acquisition and the stereo analysis. Different methods to acquire stereo images exist. Research currently follows the three following approaches:

- Dual-beam scanning electron microscope
- Specimen table tilting
- SEM beam deflection

The first two approaches have some disadvantages. Dual-beam scanning microscopes are very expensive and far away from being the standard in most SEM environments. A standard specimen table is already able to perform the required shift and tilt movements for the second method, but the experimental

setup of many applications is not compatible with the tilting of the specimen table, e.g. setups for manipulation processes with mobile robots. These are core reasons why our group follows the approach of electron beam deflection (see also in (Jahnisch and Fatikow, 2007)). The beam is deflected by two units:

- Internal SEM beam shift unit
- External self-built-magnetic lens

The advantage of this setup is the easy integration of the system into standard SEMs.

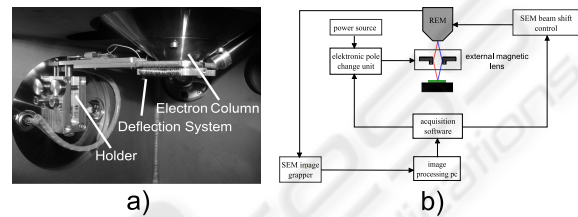


Figure 8: a) An image of the integrated external magnetic lens in the SEM vacuum chamber. b) A sketch of the principle of electron beam deflection and the control system of the stereo image acquisition in the SEM.

To acquire stereo images, special software was written to synchronize the SEM beam shift control and the external magnetic lens. Figure 8 shows the principle and control flow of the stereo image acquisition. The disadvantage and main difference of stereoscopy in the SEM to macro world stereoscopy is the small vergence angle due to technical limits imposed by the construction of the acquisition system. This is one of the reasons why there are special requirements to the stereo image analysis in the SEM. The main challenge of the analysis is to solve the correspondence problem. The solution is derived by finding the corresponding points or objects in the stereo image pair.

Currently there are just a few analysis methods to solve correspondence in the scanning electron microscopy. The algorithm used in our vision feedback group (see (Jahnisch and Fatikow, 2007)) is based on the human visual cortex and is able to calculate disparities without any previous knowledge of the specimen. This procedure is a pixel-based correspondence solving algorithm. On the one hand this method is very versatile, but on the other hand the algorithm needs almost noise free stereo input images and a very long computation time to create reliable disparities. Current research is looking for new methods to calculate the correspondence in SEM stereo images with the following features:

- Fast calculation for real-time applications
- High noise robustness

- High reliability and accuracy for automation applications

Feature-based correspondence analysis is interesting due to its flexibility. Therefore, common methods for image tracking, recognition and classification are reviewed with respect to their capability of calculating correspondence under SEM-specific conditions. Due to the experience with the application of active contours (see section 3) in SEM applications, their high noise robustness and the fast calculation time after an initialization step, they are a promising candidate for correspondence analysis. The principle is to initialize the active contour based tracking algorithm on one of the two stereo images and use the derived contour to initialize the tracking algorithm on the other stereo image. Due to the small vergence angle and the small acquisition time difference of a stereo image pair the correspondence between objects can be solved.

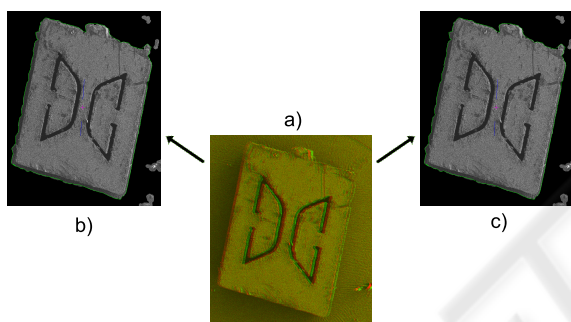


Figure 9: a) Shows the red green image of the stereo image pair. b) Preprocessed left image with active contour. c) Preprocessed right image with active contour initialized by the right image contour.

In the following step, the center points and the orientations of both contours are used to calculate the disparity and to calculate the angle difference between the contours. This difference reflects the z position and orientation of the specimen. To validate this new procedure, a series of stereo images with different z-positions of a specimen in the SEM were taken. The following two diagrams show two series of measurement with different SEM scan speeds.

Figure 10 shows a series of small z-differences with their corresponding disparities. Due to the small magnification of 60x the resolution of the stereo images is insufficient to detect disparities to z-displacements of a few μm . That is the reason for the noise with small displacements. Thanks to the features of SEMs and the scalability of the active contours algorithm, the disparity calculation of small z-displacement is still possible in high magnifications.

This new feature-based correspondence problem is just limited by the resolution and the vergence an-

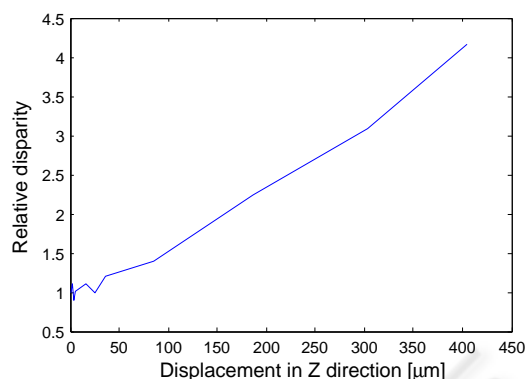


Figure 10: Graph shows small z-displacements with corresponding disparities.

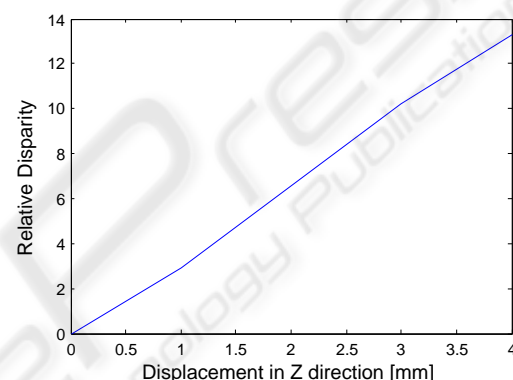


Figure 11: Graph shows z-displacements in the range of 0,5 to 4 mm with corresponding disparities.

gle. Recently, the algorithm was tested with CNTs using a magnification of 1000x with the ability to detect z displacement in the single-digit μm domain. In the future, it is planned to build a new SEM scan generator to increase the stereo image resolution and to build new lens systems to get a higher vergence angle.

5 SUMMARY

In this paper, we have shown a new approach for depth estimation using SEM images. The use of a duplicated two-dimensional tracking algorithm generates data which can be used to determine depth. The algorithm is initialized and then duplicates the contour information to process both images from a stereo image pair. The displacements detected are a measure of depth. The results of this algorithm are very promising and further effort will be made to improve the approach. Even with the results obtained already, the featured algorithm shows to be a promising tool for the automation of nanohandling processes. With

magnifications as low as 60x which has been used in this experiment, depth differences in the order of $50\mu\text{m}$ can be detected.

REFERENCES

- Blake, A. and Isard, M. (2000). *Active Contours*. Springer.
- Forsyth, D. and Ponce, J. (2002). *Computer Vision: A Modern Approach*. Prentice Hall.
- Gonzalez and Woods (2008). *Digital Image Processing*. Prentice Hall.
- Jaehne, B. (1991). *Digital Image Processing*. Springer.
- Jahnisch, M. and Fatikow, S. (2007). 3-D vision feedback for nanohandling monitoring in a scanning electron microscope. *International Journal of Optomechatronics*, 1(1):4–26.
- Kass, M., Witkin, A., and Terzopoulos, D. (1988). Snakes: Active contour models. *International Journal of Computer Vision*, 1(4):321–331.
- Kratochvil, B. E., Dong, L. X., and Nelson, B. J. (2007). Real-time rigid-body visual tracking in a scanning electron microscope. In *Proc. of the 7th IEEE Conf. on Nanotechnology (IEEE-NANO2007), Hong Kong, China*.
- Sievers, T. (2006). Global sensor feedback for automatic nanohandling inside a scanning electron microscope. In *Proc. of 2nd I*PROMS NoE Virtual International Conference on Intelligent Production Machines and Systems*, pages 289–294.
- Sievers, T. (2007). *Echtzeit-Objektverfolgung im Rasterelektronenmikroskop*. PhD thesis, University of Oldenburg.
- Sievers, T. and Fatikow, S. (2006). Real-time object tracking for the robot-based nanohandling in a scanning electron microscope. *Journal of Micromechatronics*, 3(3-4):267–284.

